Available online at www.sciencedirect.com

ScienceDirect

Spectrochimica Acta Part A 71 (2008) 669–675

SPECTROCHIMICA ACTA PART A

www.elsevier.com/locate/saa

Spectral and thermal studies with anti-fungal aspects of some organotin(IV) complexes with nitrogen and sulphur donor ligands derived from 2-phenylethylamine

Rajeev Singh, N.K. Kaushik *

Organometallic Research Laboratory, Department of Chemistry, University of Delhi, Delhi-110007, India

Received 19 April 2007; received in revised form 5 January 2008; accepted 12 January 2008

Abstract

Some complexes of 2-phenylethyl dithiocarbamate, thiohydrazides and thiodiamines with dibenzyltin(IV) chloride, tribenzyltin(IV) chloride and di(*para*-chlorobenzyl)tin(IV) dichloride have been synthesized and investigated in 1:2 and 1:1 molar ratio. The dithiocarbamate ligand act as monoanionic bidentate and thiohydrazide, thiodiamines act as neutral bidentate ligand. The synthesized complexes have been characterized by elemental analysis and molecular weight determination studies and their bonding pattern suggested on the basis of electronic, infrared, ^{1}H and ^{13}C NMR spectroscopy. Using thermogravimetric (TG) and differential thermal analysis (DTA) various thermodynamic and kinetic parameters *viz.* reaction order (n), apparent activation energy (E_a), apparent activation entropy ($S^\#$) and heat of reaction (ΔH) have been calculated and correlated with the structural aspects for solid-state decomposition of complexes. The ligands and their tin complexes have also been screened for their fungitoxicity activity against *Rhizoctonia solanii* and *Sclerotium rolfsii* and their ED_{50} values calculated.

Keywords: Organotin(IV) complexes; Synthesis; Spectral; Phenomenological; Kinetic; Anti-fungal (ED_{50})

1. Introduction

Organotin compounds have a wide range of applications and they are amongst the most widely used organometallic chemicals. The use of organotins in industry has risen dramatically as a result of their wide range of technical applications and their favorable environmental and toxological properties [1]. At present, the industrial uses of non-toxic organotin compounds account for almost two-third of the total world consumption, though the other major use for these derivatives as anticancer [2], antifouling [3,4] and bactericidal [5,6], fungicidal [7–9] and antiviral agents [10].

The dithiocarbamates ($R_2NCS_2^-$) are the half-amides of dithiocarbonic acid. These are the sulphur analogs of carbamates ($R_2NCO_2^-$). The strong metal binding properties of dithiocarbamates are directly related to their possession of two donor sulphur atoms. DTCs are the main group of fungicides used to control approximately 400 pathogens of more than 70 crops and are registered in all the EU member states and many other countries [11]. The thiohydrazides are the hydrazine derivatives of dithioacid ($RCS_2^-H^+$) and thiodiamines are the diamine derivatives of dithioacid ($RCS_2^-H^+$). The work has been reported by many workers [7,8,11–17] by synthesizing and characterizing these types of ligands and their complexes using different metals. In this paper we report on the synthesis, spectral characterization, thermal decomposition pattern and the fungitoxicity aspects of the reaction of organotin(IV) chloride with the ligands proposed, derived from 2-phenylethylamine. The structures of the ligands are shown in Figs. 1 and 2.

2. Experimental

2.1. Physical measurements

All reagents used were AR grades and the solvents were purified by standard method and dried before use. The elemental analysis was carried out on an Elementar Analysensysteme GmbH Varion EL *III*, Germany. Tin was estimated gravimetrically as SnO_2 and chlorine was estimated volumetrically by Volhard's method. The Rast Camphor Method was used to carry

---

* Corresponding author. Tel.: +91 931 122 5501; fax: +91 112 776 2780.
E-mail addresses: raajeevssiingh@yahoo.com (R. Singh), narenderkumar_kaushik@yahoo.co.in (N.K. Kaushik).

1386-1425/$ – see front matter © 2008 Elsevier B.V. All rights reserved.
doi:10.1016/j.saa.2008.01.015

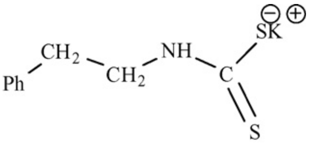

Fig. 1. Structure of dithiocarbamate ligand (L^1).

out the molecular weight determinations. The electronic spectra were recorded on a Varian Cary 100 UV–vis spectrophotometer. IR and far IR spectra were recorded on KBr and polyethylene discs respectively using a PerkinElmer Spectrum 2000 FTIR spectrometer and ^1H, ^{13}C NMR spectra were recorded on a Bruker Spectrospin Advance 300 spectrometer. The TG/DTA were recorded on a Thermoflex PTC-10A Rigaku Corporation, Japan in static air at heating rate 5° min^{-1}. The Pt crucible was used with alumina as the reference material.

2.3.1. Preparation of 2-phenylethyl dithiocarbamate (L^1)

The dithiocarbamate was prepared by the method described by Gilman and Blatt [20] with some modifications. Phenylethylamine (25.37 ml, 0.2 mol) (density 0.960) was dissolved in ethanol and to it KOH (11.2 g, 0.2 mol) in minimum ethanol was added. Carbon disulphide (12.06 ml, 0.2 mol) (density 1.26) was then added to the mixture, the temperature being kept below 10 °C. An off-white crystalline precipitate of the potassium salt of 2-phenylethyl dithiocarbamate separated, which was further recrystallized from ethanol and dried in vacuum dessicator over $CaCl_2$.

Anal. Calcd. for L^1 (%): C, 45.92; H, 4.28; N, 5.95; Found: C, 44.92; H, 4.78; N, 5.55.

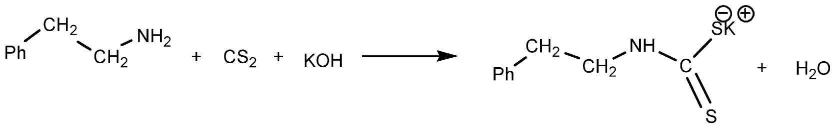

2.2. Fungitoxicity testing

The *in vitro* antifungal activities of the ligands and their corresponding complexes were tested by poisoned food technique using potato–dextrose–agar (PDA) medium at 500 ppm, 250 ppm and 125 ppm. *Rhizoctonia solanii* Kuhn and *Sclerotium rolfsii* Saccardo were used as test organisms. A 5-mm thick disk of fungus (spores and mycelium) cut from earlier subcultured Petridish was put in the centre of the solidified medium in the test Petriplates and lids replaced. Both treated and control Petriplates were kept in BOD incubator at 25 ± 1 °C for 4–6 days. The mycellial growth of fungus (cm) in both treated (T) and control (C) Petriplates were measured diametrically in three different directions. Two replicates were taken for each treatment. From the mean growth of above reading percentage inhibition of growth (I) was calculated by using formula: $I(\%) = \{[C - T]/C\} \times 100$. From the mean growth percentage inhibition ($\%I$), the ED_{50} values were calculated by means of a Basic LD_{50} programme Version 1.1 [18].

2.3. Preparation of organotin and ligands

Dibenzyltin(IV) dichloride $(C_6H_5CH_2)_2SnCl_2$; di(*para*-chlorobenzyl)tin(IV) dichloride $(p\text{-}ClC_6H_4CH_2)_2SnCl_2$ and tribenzyltin(IV) chloride $(C_6H_5CH_2)_3SnCl$ were synthesized by the method given by Sisido et al. [19].

2.3.2. Preparation of N-thiohydrazide (L^2) and N-thiodiamine (L^3 and L^4)

The ligand 2-phenylethyl *N*-thiohydrazide have been synthesized by the method of Kazakova et al. [21–23] with some modifications. The aqueous solution of dithiocarbamate was treated with freshly prepared potassium chloroacetate (0.2 mol). The temperature of the reaction mixture was increased to and maintained below 40 °C for 1 h. The mixture was then left for 24 h at room temperature. Then a methanolic solution of hydrazine hydrate (9.72 ml, 0.2 mol) was added and the reaction mixture heated on a water bath for an hour, at which the desired product separated. It was cooled in ice for 24 h, and then filtered. The thiohydrazide so obtained was recrystallized and dried. Similar procedure was followed for *N*-thiodiamines of 1,3-diaminopropane (L^3) and 1,2-diaminoethane (L^4). They were recrystallized from water and dried over $CaCl_2$.

Anal. Calcd. for L^2 (%): 55.38; H, 6.66; N, 21.53; Found: C, 54.37; H, 6.65; N, 20.44.

Anal. Calcd. for L^3 (%): C, 60.75; H, 8.01; N, 17.73; Found: C, 61.30; H, 7.82; N, 17.77.

Anal. Calcd. for L^4 (%): C, 59.19; H, 7.65; N, 18.83; Found: C, 59.5; H, 6.32; N, 18.73.

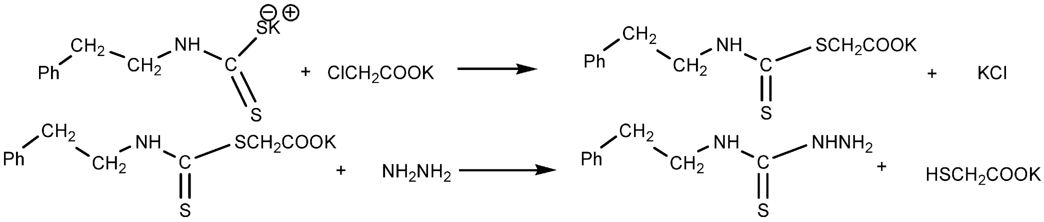

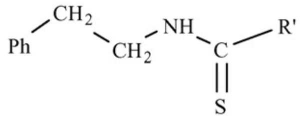

Fig. 2. Structure of *N*-thiohydrazide and *N*-thiodiamine ligands. R′: L^2, $-NHNH_2$; L^3, $-NH(CH_2)_3NH_2$; L^4, $-NH(CH_2)_2NH_2$.

2.4. Preparation of complexes

2.4.1. Preparation of dithiocarbamate complexes

A solution of potassium 2-phenylethyl dithiocarbamate [L^1, 4.70 g (0.02 mol)] in 25 ml THF was added slowly to a solution of R_2SnCl_2 (0.01 mol) or R_3SnCl (0.02 mol) in 25 ml THF. The contents were stirred for ∼9 h on a water bath at 60 °C. The solution was reduced in concentration to one-fourth of original volume under vacuum and the complex so obtained was dried in a vacuum dessicator over anhydrous $CaCl_2$.

2.4.2. Preparation of N-thiohydrazide and N-thiodiamines complexes

A solution of ligand [L^2, 3.90 g; L^3, 4.74 g; L^4, 4.46 g (0.02 mol)] in 25 ml of dioxane was added slowly with continuous stirring to corresponding organotin chloride R_2SnCl_2 or R_3SnCl (0.02 mol) in 25 ml of dioxane. The mixture so obtained was refluxed for an hour and stirred for additional ∼4 h and then the solution was reduced in concentration to one-fourth of its original volume under vacuum. The complex so obtained was recrystallized in acetone and finally washed with petroleum ether and dried in a dessicator over $CaCl_2$. For the $(C_6H_4CH_2)_2Sn(L^3)Cl_2$ complex, 1:7 distilled water–acetone mixture was used as a solvent medium.

3. Results and discussions

The complexes synthesized were found to be pure and soluble in acetone, chloroform and dimethylsulphoxide solvents. All the complexes were colored and showed sharp melting point. The elemental analysis is given for the complexes in Table 1.

3.1. Electronic spectra

In the UV–vis spectra, the dithiocarbamate ligand showed two absorption bands due to the chromophore group (NCS_2). Band I in the 260 nm region is attributed to π–π* transition of $N \underline{\cdots} C \underline{\cdots} S$ groups. Band II in the ∼290 nm region is due to π–π* electronic transition involving lone pair of electrons located on the sulphur atom, respectively. On complexation these bands shifted to lower wavelength, showing the involvement of NCS_2 group in all the complexes. In case of thiohydrazide and thiodiamines due to chromophore region, absorption bands are assigned as π–π* transition. These bands are at ∼262 nm corresponding to free ligands which shift to lower wavelength ∼261 nm indicating the involvement of C=S group on complexation. One additional band also appears in the complexes because of metal–ligand charge transfer.

Table 1
Synthesis and characterization of organotin(IV) complexes

Compounds	Ligand	Molar ratio	Product, color and state	Empirical formula	Analysis found (Calc.) (%)						Mol. wt. Found (Calc.)
					Sn	C	H	N	S	Cl	
$(C_6H_5CH_2)_2SnCl_2$	L^1	1:2	$(C_6H_5CH_2)_2Sn(L^1)_2$, yellow, semi-solid	$C_{32}H_{34}SnN_2S_4$	17.92 (17.22)	55.99 (55.51)	5.01 (4.91)	4.42 (4.44)	19.99 (18.50)		689.93 (694.06)
$(p\text{-}ClC_6H_4CH_2)_2SnCl_2$	L^1	1:2	$(p\text{-}ClC_6H_4CH_2)_2Sn(L^1)_2$, dark yellow, semi-solid	$C_{32}H_{32}SnN_2S_4Cl_2$	15.56 (15.77)	50.89 (50.51)	4.98 (4.33)	3.99 (3.77)	16.78 (16.89)	10.09 (9.20)	757.03 (762.81)
$(C_6H_5CH_2)_3SnCl$	L^1	1:1	$(C_6H_5CH_2)_3Sn(L^1)$, yellow, sticky solid	$C_{30}H_{31}SnNS_2$	21.11 (20.27)	61.66 (61.24)	5.66 (5.51)	3.01 (2.48)	9.99 (10.91)		581.36 (588.41)
$(C_6H_5CH_2)_2SnCl_2$	L^2	1:1	$(C_6H_5CH_2)_2Sn(L^2)Cl_2$, yellow, solid	$C_{23}H_{27}SnN_3SCl_2$	19.99 (20.96)	48.48 (48.75)	4.92 (4.87)	8.21 (7.51)	4.92 (5.66)	12.63 (12.59)	557.11 (566.03)
$(C_6H_5CH_2)_2SnCl_2$	L^3	1:1	$(C_6H_5CH_2)_2Sn(L^3)Cl_2$, brown, solid	$C_{26}H_{33}SnN_3SCl_2$	18.56 (19.89)	51.51 (51.59)	5.89 (5.87)	7.29 (6.59)	5.75 (5.66)	11.55 (11.78)	607.33 (610.34)
$(C_6H_5CH_2)_2SnCl_2$	L^4	1:1	$(C_6H_5CH_2)_2Sn(L^4)Cl_2$, rust brown, solid	$C_{25}H_{31}SnN_3SCl_2$	19.29 (19.89)	49.29 (50.85)	5.99 (5.55)	7.89 (7.55)	5.21 (5.45)	11.90 (11.78)	590.78 (597.06)

Table 2
^1H and ^{13}C NMR spectral data for dithiocarbamate complexes

Complexes	^1H		^{13}C	
	—NH	—Sn—CH$_2$—	—C=S	—Sn—CH$_2$
L^1	3.61	–	179.9	–
$(C_6H_5CH_2)_2Sn(L^1)_2$	3.81	2.89	181.5	18.19
$(p\text{-}ClC_6H_4CH_2)_2Sn(L^1)_2$	3.83	2.93	186.6	24.66
$(C_6H_5CH_2)_3Sn(L^1)$	3.89	2.91	183.5	17.34

3.2. Infrared spectra

The IR spectra of dithiocarbamate complexes show a strong band in the 1491–1505 cm^{-1} region, which is attributed to the ν(C=N) stretching frequency. In the free ligands the ν(C=N) frequency occurs at ~1452 cm^{-1}. The occurrence of this frequency at lower energy in the free ligands as compared to the metal complexes is expected since on complexation there is an increase in electron density on the sulphur atoms due to back donation of electrons from metal d-orbitals to the vacant antibonding sulphur orbitals. The band at 950 cm^{-1} and 933 cm^{-1} is assigned to ν(C=S) which on complexation shows a strong band at 1007 cm^{-1} indicating that all the dithiocarbamate ligands are of bidentate nature and symmetrically bonded.

Comparatively in thiohydrazide and thiodiamines complexes, the ⟩NH stretching vibration at ~3210 cm^{-1} of terminal ⟩NH$_2$ group shifted to lower frequency, indicating the coordination of –NH$_2$ group to the metal atom. The band at 933 cm^{-1} assignable to a ν(C=S) shifts to lower frequency ~903 cm^{-1}. A peak at 1207 cm^{-1} is observed for ν(C–N). Significant changes in ligand bands upon complexation indicate coordination through the terminal nitrogen and thiocarbonyl sulphur. Besides this, far IR spectra of the metal complexes showed several new bands, which are ν(Sn–S) [24,25] at 352 cm^{-1}, ν(Sn–N) [25,26] at 696 cm^{-1}, ν(Sn–Cl) [24,25] at 375 cm^{-1}, thus lending support to the proposed coordination in the complexes.

3.3. ^1H NMR spectra

The proton magnetic resonance spectra of the ligands and their corresponding 1:2 and 1:1 tin complexes were recorded in CDCl$_3$ and shown in Tables 2 and 3. The results were compared with, those of the free ligands. A number of signals have been observed which on complexation shifts from their original position. A downfield shift in the resonance signals of the complexes in comparison to the free ligands is due to coordination of the ligand to metal ion.

Table 3
^1H and ^{13}C NMR spectral data for thiohydrazide and thiodiamine complexes

Complexes	^1H		^{13}C	
	—NH$_2$	—Sn—CH$_2$—	—C=S	—Sn—CH$_2$—
L^2	3.52	–	178.33	–
$(C_6H_5CH_2)_2Sn(L^2)Cl_2$	3.89	2.91	181.45	19.43
L^3	3.65	–	180.09	–
$(C_6H_5CH_2)_2Sn(L^3)Cl_2$	3.77	2.91	188.30	20.44
L^4	3.69	–	180.09	–
$(C_6H_5CH_2)_2Sn(L^4)Cl_2$	3.76	2.96	182.33	21.00

In thiohydrazides and thiodiamines (Table 3), the terminal –NH$_2$ of the thiohydrazide ligand experiences a downfield shift indicating coordination through the terminal nitrogen or NH$_2$ group to the tin metal. The aromatic proton signals, which appear in the form of a complex multiplet at δ 6.89–6.78 ppm, shifts to δ 6.92–6.79 ppm due to deshielding on complexation. On complexation, additional peaks were also observed in the region δ 7.20–7.11 ppm (ArH) and δ ~2.91 ppm corresponding to the –Sn–CH$_2$– groups present in the complexes. On comparison with literature reports [12,14] of similar synthesized compounds, significant changes in the δ (ppm) value support more stable coordination on complexation.

3.4. ^{13}C NMR spectra

^{13}CNMR data have been recorded for all the ligands and their corresponding tin complexes (Tables 2 and 3). In all the complexes, the thione carbon suffer upfield shifts in the complexes thereby supporting a change in the ⟩C=S bond order indicating that the coordination of ligands is through sulphur to the metal ions.

On the basis of elemental analysis, spectral evidence and thermal data; the following structures representing coordination have been proposed for the complexes synthesized (Figs. 3 and 4).

3.5. Thermal studies

3.5.1. Phenomenological aspects

The phenomenological data for every step, determined from the TG curves are presented in Table 4.

$(C_6H_5CH_2)_2Sn(L^1)_2$ complex. The TG curve (Fig. 5, curve A) shows that the complex starts decomposing at 380 K and continues to decompose till 566 K, this step corresponds to

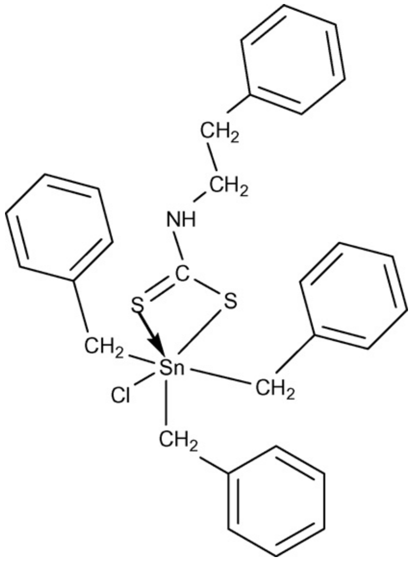

Fig. 3. Dithiocarbamate complexes.

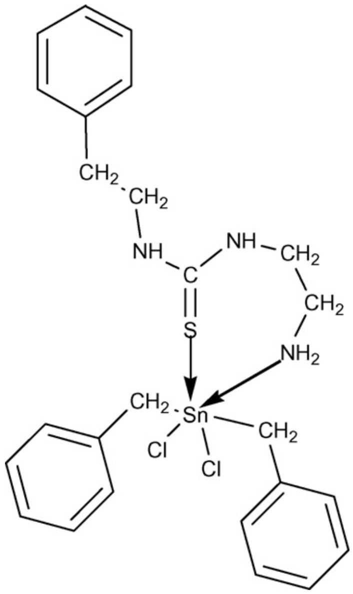

Fig. 4. *N*-Thiodiamine complexes.

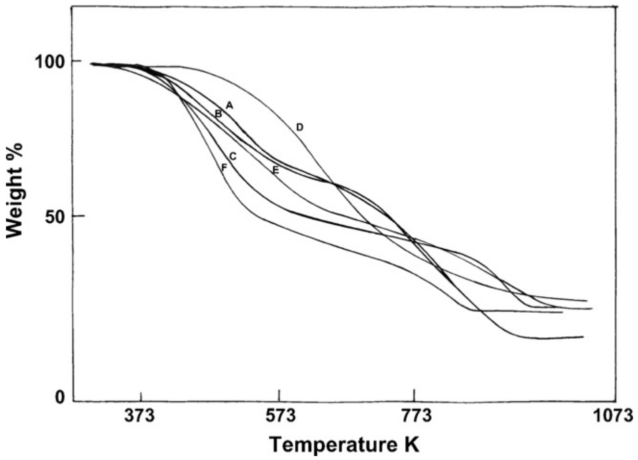

Fig. 5. TG curves for dithiocarbamate complexes: (A) $(C_6H_5CH_2)_2Sn(L^1)_2$, (B) $(p\text{-}ClC_6H_4CH_2)_2Sn(L^1)_2$, (C) $(C_6H_5CH_2)_3Sn(L^1)$, (D) $(C_6H_5CH_2)_2Sn(L^2)Cl_2$, (E) $(C_6H_5CH_2)_2Sn(L^3)Cl_2$ and (F) $(C_6H_5CH_2)_3Sn(L^4)Cl_2$.

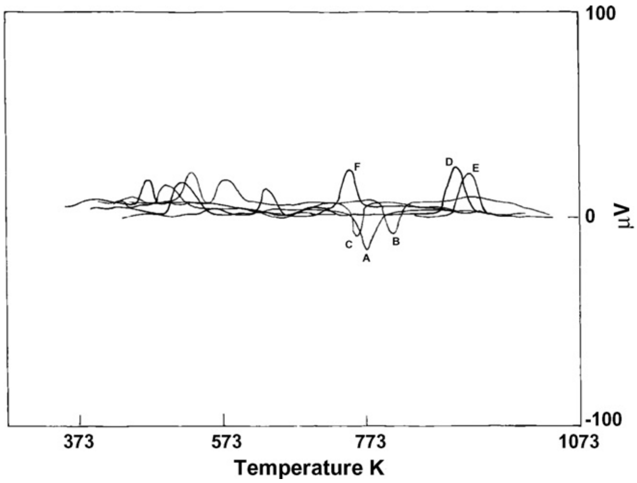

Fig. 6. DTA curves for dithiocarbamate complexes: (A) $(C_6H_5CH_2)_2Sn(L^1)_2$, (B) $(p\text{-}ClC_6H_4CH_2)_2Sn(L^1)_2$, (C) $(C_6H_5CH_2)_3Sn(L^1)$, (D) $(C_6H_5CH_2)_2Sn(L^2)Cl_2$, (E) $(C_6H_5CH_2)_2Sn(L^3)Cl_2$ and (F) $(C_6H_5CH_2)_3$ $Sn(L^4)Cl_2$.

the loss of the two benzyl groups. The expected and observed mass losses are 26.27% and 25.25% respectively. The final step corresponding to the decomposition of organic part L^1 and subsequent conversion of Sn to SnO_2 lies in the temperature range 566–890 K. The total expected and observed mass losses, after the complete formation of SnO_2 are 78.24% and 77.39% respectively. In the DTA profile (Fig. 6, curve A) step I is shown as an exothermic peak $T_{max} = 478$ K and the final step is marked by an endothermic peak with $T_{max} = 777$ K. The heat of reaction (ΔH) for step I is 19.00 kJ g^{-1} and for the step II it is 62.36 kJ g^{-1}.

$(C_6H_5CH_2)_3Sn(L^1)$ complex. Step I of thermal degradation, which initiated at 410 K and continued up to 559 K corresponds to the loss of all the three benzyl groups (Fig. 5, curve C). The expected and observed mass losses were 46.45% and 45.44% respectively. After the completion of the final step, which corresponded to the decomposition of the organic part L^1 and the formation of SnO_2, the total expected and observed mass losses were 73.83% and 74.35%, respectively. This step lies in the temperature range 559–930 K. The TG curve is shown in Fig. 1 curve C. The DTA profile (Fig. 6, curve C) showed two thermal effects.

Table 4
Phenomenological data for the thermal decomposition of the complexes

Complexes	Step no.	TG plateaux (K)	Mass loss observed (calc.) %	Nature of product
$(C_6H_5CH_2)_2Sn(L^1)_2$	I	380–566	25.25 (26.27)	Loss of two benzyl groups and chlorine atom
	II	566–890	77.39 (78.24)	Formation of SnO_2
$(p\text{-}ClC_6H_4CH_2)_2Sn(L^1)_2$	I	389–610	31.50 (32.90)	Loss of two *p*-chlorobenzyl groups and two chlorine atoms
	II	610–920	79.8 (80.22)	Formation of SnO_2
$(C_6H_5CH_2)_3Sn(L^1)$	I	410–559	45.44 (46.45)	Loss of three benzyl groups and chlorine atom
	II	559–930	73.83 (74.35)	Formation of SnO_2
$(C_6H_5CH_2)_2Sn(L^2)Cl_2$	I	423–690	43.29 (44.64)	Loss of two benzyl groups and chlorine atom
	II	690–1010	72.91 (73.40)	Formation of SnO_2
$(C_6H_5CH_2)_2Sn(L^3)Cl_2$	I	344–596	40.24 (41.62)	Loss of two benzyl groups and chlorine atom
	II	596–999	74.34 (75.91)	Formation of SnO_2
$(C_6H_5CH_2)_2Sn(L^4)Cl_2$	I	375–533	41.55 (42.47)	Loss of two benzyl groups and chlorine atom
	II	533–863	73.25 (74.60)	Formation of SnO_2

Table 5
Kinetic parameters for the thermal decomposition of the complexes

Complexes	Step no.	TG			DTA		
		n	E_a (kJ mol^{-1})	S (J K^{-1} mol^{-1})	Thermal effect	T_{max} (K)	ΔH (kJ g^{-1})
$(C_6H_5CH_2)_2Sn(L^1)_2$	I	1	34.60	4.15	Exo	478	19.00
	II	1	55.63	3.57	Endo	777	62.36
(p-$ClC_6H_4CH_2)_2Sn(L^1)_2$	I	1	33.63	2.50	Exo	560	14.23
	II	1	60.76	4.16	Endo	792	70.29
$(C_6H_5CH_2)_3Sn(L^1)$	I	1	39.68	4.63	Exo	515	9.64
	II	1	49.17	2.80	Endo	756	71.56
$(C_6H_5CH_2)_2Sn(L^2)Cl_2$	I	1	34.40	1.73	Exo	630	14.33
	II	1	71.14	4.30	Exo	901	48.63
$(C_6H_5CH_2)_2Sn(L^3)Cl_2$	I	1	27.45	2.12	Exo	492	24.63
	II	1	50.67	1.65	Exo	892	47.48
$(C_6H_5CH_2)_2Sn(L^4)Cl_2$	I	1	41.25	5.99	Exo	471	9.81
	II	1	45.51	2.29	Exo	750	51.63

The exothermic peak with T_{max} at 515 K ($\Delta H = 9.64$ kJ g^{-1}) corresponded to step I and an endothermic peak with T_{max} at 756 K ($\Delta H = 71.56$ kJ g^{-1}) corresponded to the final step.

$(C_6H_5CH_2)_2Sn(L^2)Cl_2$ complex. The TG curve (Fig. 5, curve D) for this complex shows that almost 43.29% mass loss occurs up to 690 K. The initial thermal decomposition step is over the range 423–690 K. At this step there is loss of two benzyl groups and chlorine atoms. The subsequent step at 1010 K shows a mass loss of 72.90%; tin oxide (SnO_2) is the end product. The DTA curve (Fig. 6, curve D) show an exothermic peak at $T_{max} = 630$ K ($\Delta H = 14.33$ kJ g^{-1}), for step I. An exothermic peak at 901 K ($\Delta H = 48.63$ kJ g^{-1}) corresponds to complete decomposition of the complex.

3.5.2. Kinetic aspects

The kinetics of thermal decomposition of these complexes has been measured under dynamic temperature conditions. Evaluation of kinetic parameters has been performed by means of the Horowitz–Metzger method [26] assuming a rate law of the type $dx/dt = K(1-\alpha)^n$ and an Arrhenius equation of the type $K = Z e^{-E/RT}$ to be valid, where α represents the fraction transformed, n the order of reaction, K the rate constant and E is the activation energy; the graph for $\log(-\ln(1-\alpha))$ versus $1/T \times 10^3$ gave straight lines with slope $E\theta/2.303T_m^2$, where θ is a reference temperature, $T - T_m$, T_m is the peak temperature. From the TG curves, the order of reaction (n), activation energy (E_a) and entropy of activation ($S^{\#}$) of the thermal decomposition reaction have been elucidated. The values of the heat of reaction ΔH, microvolts, were obtained directly from the computer fitted to the thermoanalyser; it was converted to kJ g^{-1}. The various kinetic parameters calculated are given in Table 5.

3.5.3. Discussions

The TG and DTA curves are shown in Figs. 5 and 6, respectively. The order of reaction for the thermal decomposition of the above complexes was one. The decomposition of the complexes was observed to be a two-step process, step 1 corresponding to the loss of all the benzyl groups (and chlorine atom too in case of di(p-chlorobenzyltin(IV) dichloride). Step II corresponded to the decomposition of the organic part, L and ultimately, formation of SnO_2. The DTA profile of each complex showed the corresponding exothermic or endothermic peak. Further it was observed from the above data, that the Sn–R bond (where R = benzyl/p-chlorobenzyl) and Sn–Cl bond is weaker than Sn–L (L = ligand) bond so these bonds cleave before Sn–L bond and hence, the activation energy (E_a) value for step I is lower than step II because of greater steric hindrance initially in the complexes. The energy of

Table 6
Anti-fungal screening data of the ligands and their tin complexes. (Inhibition %) (Conc. 125, 250, 500 ppm)

Compound	*Rhizoctonia solanii*				*Sclerotium rolfsii*			
	125	250	500	ED_{50}	125	250	500	ED_{50}
L^1	28.32	54.64	62.31	54.82	46.14	59.36	64.18	30.83
$(C_6H_5CH_2)_3Sn(L^1)Cl$	52.66	68.86	73.31	19.76	45.23	54.66	68.29	35.40
(p-$ClC_6H_4CH_2)_2Sn(L^1)Cl_2$	43.23	58.44	68.21	35.09	42.38	55.55	75.45	35.60
L^2	37.91	57.18	66.66	42.62	29.33	64.86	78.82	39.48
$(C_6H_5CH_2)_2Sn(L^2)Cl_2$	43.33	63.20	83.40	31.76	47.51	62.99	83.98	29.10
L^3	25.25	43.62	78.52	51.26	36.82	43.28	68.92	54.34
$(C_6H_5CH_2)_2Sn(L^3)Cl_2$	39.36	55.65	73.65	39.38	41.36	61.14	78.36	33.15
L^4	55.70	63.56	79.26	21.21	46.68	59.15	65.55	31.17
$(C_6H_5CH_2)_2Sn(L^4)Cl_2$	43.2	60.60	77.32	33.11	48.72	57.88	75.12	28.86

activation, in turn, reflected the kinetic liability of the complexes.

3.6. Anti-fungal studies

The results reported in table reveal that the tin complexes with these ligands are much more active than the parent ligand against the same microorganisms. With increase in concentration of the compounds there occurs increase in percentage of inhibition. Higher concentration proves inhibitory for fungal growth (Table 6).

Acknowledgements

The authors thank Dr. R.L. Gupta and Bijul Lakshman A, Divison of Agricultural Chemicals, Indian Agricultural Research Institute (IARI), Pusa, New Delhi for the antifungal studies of the compounds and University Scientific Instrumentation Center (USIC), University of Delhi, India for TG/DTA studies.

References

[1] A.G. Davies, P.J. Smith, Adv. Inorg. Chem. Radiochem. 23 (1980) 1–77.
[2] P.M. Samuel, Dick de Vos, D. Raveendra, J.A.R.P. Sarma, S. Roy, Bioorg. Med. Chem. Lett. 12 (2002) 61–64.
[3] D.C. Cinito Roberto, D.C. Giorgio, Chem. Abstr. 120 (1994) 156632.
[4] A.G. Davies, Organotin Chemistry, 2nd edn., Wiley VCH, Weinheim, 2004, pp. 383.
[5] M. Ashfaq, M.I. Khan, M.K. Baloch, A. Malik, J. Organomet. Chem. 689 (2004) 238–245.
[6] A. Bacchi, A. Bonardi, M. Carcelli, P. Mazza, P. Pelagatti, C. Pelizzi, G. Pelizzi, C. Solinas, F. Zani, J. Inorg. Biochem. 69 (1998) 101–112.
[7] R.V. Singh, P. Chaudhary, K. Poonia, S. Chauhan, Spectrochim. Acta A 70 (2008) 587–594.
[8] Rajeev Singh, N.K. Kaushik, Spectrochim. Acta A 65 (2006) 950–954.
[9] A. Bacchi, M. Carcelli, P. Pelagatti, G. Pelizzi, M.C. Rodriguez-Arguelles, D. Rogolino, C. Solinas, F. Zani, J. Inorg. Biochem. 99 (2005) 397–408.
[10] M. Nath, S. Goyal, Met.-Based Drugs 2 (1995) 297.
[11] R. Sharma, N.K. Kaushik, Ind. J. Chem. 43A (2004) 769–772.
[12] J. Reena, N.K. Kaushik, J. Therm. Anal. 49 (1997) 713–725.
[13] N.K. Kaushik, A.K. Mishra, Ind. J. Chem. 42A (2003) 2762–2766.
[14] R. Singh, N.K. Kaushik, Main Group Met. Chem. 27 (2004) 327–333.
[15] F. Basuli, S.M. Peng, S. Bhattacharya, Inorg. Chem. 39 (2000) 1120–1127.
[16] E.M. Joud, A. Riou, M. Allain, M. Khan, M.A. Khan, G.M. Bouet, Polyhedron 20 (2001) 67–74.
[17] R. Charles, J.M. Ostman, W.H. Ojala, Carbohyd. Res. 337 (2002) 21–29.
[18] J.T. Trevors, Bull. Environ. Contam. Toxicol. 37 (1986) 18–26.
[19] K. Sisido, Y. Takeda, Z. Kinugawa, J. Am. Chem. Soc. 83 (1961) 538–541.
[20] H. Gilman, A.H. Blatt, Organic Synthesis, Collective Vol. I, John Wiley, New York, 1958, pp. 448.
[21] V. Ya Kazakova, Ya Partovskii, Dokl. Akad. Nauk. 134 (1960) 824.
[22] (a) K.A. Jensen, J. Prakt. Chem. 159 (1941) 189–192;
(b) K.A. Jensen, Chem. Abstr. 37 (1941) 27182.
[23] (a) D.J. Bauer, Chem. Abstr. 65 (1996) 2224e;
(b) J. Bauer, British Patent, 1026, 401 (Geo 7c, d) Welcome Foundation Ltd.
[24] K. Nakamoto, Infrared and Raman Spectra of Inorganic and Coordination Compounds, John Wiley and Sons, New York, 1997.
[25] D.J. Batyr, M.P. Starysh, V.N. Shafranskii, Y. Ya Kharitomov, Russ. J. Inorg. Chem. 19 (1974) 1517.
[26] H.H. Horowitz, G. Metzger, Anal. Chem. 35 (10) (1963) 1464–1468.